



International Journal of Innovative Research in Computer and Communication Engineering

(An ISO 3297: 2007 Certified Organization)

Website: www.ijircce.com

Vol. 5, Issue 7, July 2017

A Novel Integrated Method for Detection of Salient Regions in an Image using HDCT and Local Spatial Support by Regression

MD.Chandini¹, Dr.B.Prabhakara Rao²

M.Tech Scholar, Dept. of Electronics and Communication Engineering, UCEK (A), JNTUK, Kakinada,
Andhra Pradesh, India¹

Professor, Dept. of Electronics and Communication Engineering, UCEK (A), JNTUK, Kakinada,
Andhra Pradesh, India²

ABSTRACT: To create a saliency map of an image the first key idea is to utilize color space. This is based on an observation that salient regions often have distinctive colors compared with backgrounds in human perception, however, human perception is complicated and highly nonlinear. By mapping the low-dimensional red, green and blue color to a feature vector in a color Space. Here in this paper we utilize LUV color space technique. The CIE Luv color space is designed to be perceptually uniform, meaning that a given change in value corresponds roughly to the same perceptual difference over any part of the space. To further improve the performance of our saliency estimation, our second key idea is to utilize relative location and color contrast between super pixels as features and to resolve the saliency estimation from a tri-map via a learning-based algorithm. The experimental results on three benchmark datasets i.e., MSRA dataset, ECSSD dataset, PASCAL dataset show that our approach is effective in comparison with the previous state-of-the-art saliency estimation methods.

KEYWORDS: Salient region, Super pixel via over-segmentation, SLIC[1], Salient Tri-map, Random forest classification, color Transform technique, LUV Color space.

I. INTRODUCTION

In this paper, we propose a novel approach to automatically detect salient regions in an image so for that we have to generate tri-map initially. Our approach first estimates the approximate locations of salient regions by using a tree-based classifier. The tree-based classifier classifies each super pixel as foreground, background or unknown. The foreground and background are regions where the classifier classifies salient and non-salient regions with high confidence. The unknown regions are the regions with ambiguous features where the classifier classifies the regions with low confidence. The foreground, background and unknown regions form an initial tri-map, and our goal is to resolve the ambiguity in the unknown regions to estimate accurate saliency map. From the tri-map, we propose two different methods, [2] high-dimensional color transform (LAB and LUV) method i.e., global salient estimation [5] and local learning based method to estimate [9] the saliency map. The results of these two methods will be combined together to form our final saliency map. The overview of our method is presented in fig.1. Our algorithm is performed in super pixel level in order to reduce computations.

International Journal of Innovative Research in Computer and Communication Engineering

(An ISO 3297: 2007 Certified Organization)

Website: www.ijircce.com

Vol. 5, Issue 7, July 2017

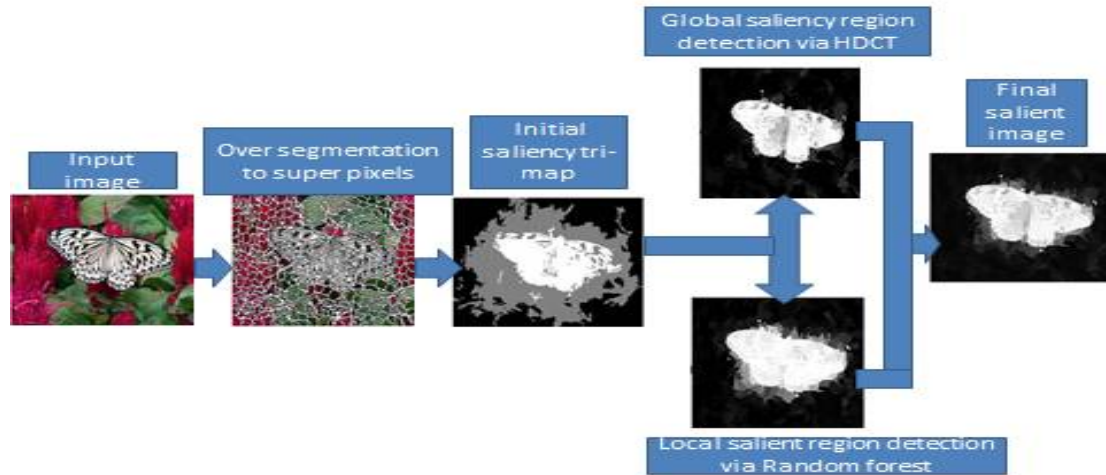


Fig 1.overview of our algorithm

II. INITIAL SALIENCY TRIMAP GENERATION

Super pixel Saliency Features:

For an input image I , we first perform over-segmentation to form super pixels $X = \{X_1, \dots, X_N\}$. We use SLIC superpixel[1] because of its low computational cost. For saliency detection we first concatenate the super pixels' x- and y-locations into our feature vector. Then we concatenate the color features. Next we concatenate histogram features. The histogram features of the superpixel DH is measured using the chi-square distance between other superpixels' histograms. where b is the number of histogram bins. In our work, we used eight bins for each histogram. For texture and shape features, we utilize the super pixel area, Histogram of gradient and singular value features[4].

$$D_H = \sum_{j=1}^N \sum_{k=1}^b [(h_{ik} - h_{jk})^2 / (h_{ik} + h_{jk})]$$

Initial Saliency Tri-map via Random Forest Classification:

After calculating the feature vectors for every super-pixel we use classification algorithm[5] to verify each region is salient or not. Here we use adaptive thresholding technique[10]. We decided whether each superpixel belongs to foreground candidate, background candidate, or unknown regions using the response value extracted from the classifier. If foreground = 1 and background = -1 then a superpixel's response value exceeds foreground, then it belongs to the foreground region; however, if the value is lower than background, then it belongs to the background region; else, it is considered as unknown. From this classification we get initial saliency Tri-map which contains foreground background and unknown regions.

III. SALIENCY ESTIMATION FROM TRIMAP

Global Saliency Estimation via LUV color space

Colors are important cues in the human visual system[6]. Many previous studies have noted that the RGB color space does not fully correspond to the space in which the human brain processes colors. It is also inconvenient to process colors in the RGB space as illumination and colors are nested here. Therefore, many different color spaces have been introduced, including YUV, YIQ, CIE Lab, and HSV. Instead of picking a particular color space for processing, we introduce a LAB and LUV color representations. Our goal is to find a linear combination of color coefficients in the HDCT space[2] such that the colors of salient regions and those of backgrounds can be distinctively separated.

International Journal of Innovative Research in Computer and Communication Engineering

(An ISO 3297: 2007 Certified Organization)

Website: www.ijirccce.com

Vol. 5, Issue 7, July 2017

Local Saliency Estimation via Regression:

F_{Si} denotes the j th nearest foreground superpixel and B_{Si} denotes the j th nearest background superpixel from the i th superpixel. Although the HDCT color space based salient region detection provides a competitive result with a low false positive rate, this method has a limitation in that it is easily affected by the texture of the salient region, and therefore, it has a relatively high false negative rate. To overcome this limitation, we present a learning-based local salient region detection that is based on the spatial and color distance from neighboring superpixels along with LUV color space representation. For saliency estimation, we used the superpixel wise random forest regression algorithm, which is effective for large high-dimensional data. It contains optimal linear combination of color values in the LUV space that results in per-pixel salient map. We extracted feature vectors using the initial tri-map. First, for each superpixel, we find the K -nearest foreground superpixels and K -nearest background superpixels. For each superpixel X_i , we find the K -nearest foreground superpixels $\mathbf{XFS} = \{XFS_1, XFS_2, \dots, XFS_K\}$ and K -nearest background superpixels $\mathbf{XBS} = \{XBS_1, XBS_2, \dots, XBS_K\}$, and we use the Euclidean distance between a superpixel X_i and superpixels \mathbf{XFS} or \mathbf{XBS} as features. The Euclidean distance [8] to the K -nearest foreground ($\mathbf{d}_{FSi} \in \mathbb{R}^{K \times 1}$) and background ($\mathbf{d}_{BSi} \in \mathbb{R}^{K \times 1}$) features of the i th superpixel and then, we estimated the saliency degree for all superpixels.

$$d_{FSi} = \begin{bmatrix} \|p_i - p_{FS_{i_1}}\|_2^2 \\ \|p_i - p_{FS_{i_2}}\|_2^2 \\ \vdots \\ \|p_i - p_{FS_{i_K}}\|_2^2 \end{bmatrix}, d_{BSi} = \begin{bmatrix} \|p_i - p_{BS_{i_1}}\|_2^2 \\ \|p_i - p_{BS_{i_2}}\|_2^2 \\ \vdots \\ \|p_i - p_{BS_{i_K}}\|_2^2 \end{bmatrix}$$

We also use the color distance features between superpixels. The feature vector of color distances from the i th superpixel to the K -nearest foreground and background superpixels is defined as follows

$$d_{CFi} = \begin{bmatrix} d(c_i, c_{FS_1}) \\ d(c_i, c_{FS_2}) \\ \vdots \\ d(c_i, c_{FS_K}) \end{bmatrix}, d_{CBi} = \begin{bmatrix} d(c_i, c_{BS_{i_1}}) \\ d(c_i, c_{BS_{i_2}}) \\ \vdots \\ d(c_i, c_{BS_{i_K}}) \end{bmatrix}$$

Final Saliency Map Generation

After we generated the global and the local saliency maps, we combined them to generate our final saliency map shown in fig.2, therefore it shows comparison of precision recall curve of each step on MSRA dataset. The examples show that the HDCT-based saliency map tends to catch the object precisely; however, the false negative rate is relatively high to textures or noise. In contrast, the learning-based saliency map is less affected by noise, and therefore, it has a low false negative rate but a high false positive rate. Therefore, combining the two maps is a significant step in our algorithm. Borji et al. [7] proposed two approaches to combine the two saliency maps. The first approach is to perform the pixelwise multiplication of the two maps, as shown below:

$$S_{mult} = \frac{1}{Z} (p(S_G) \times p(S_L))$$

The second approach is to combine the two maps using a summation:

$$S_{sum} = \frac{1}{Z} (p(S_G) + p(S_L))$$

International Journal of Innovative Research in Computer and Communication Engineering

(An ISO 3297: 2007 Certified Organization)

Website: www.ijircce.com

Vol. 5, Issue 7, July 2017

In our study, we combine the two maps more adaptively to maximize our performance. Based on summation we adopt $p(x) = \exp(x)$ as a combination function to give greater weightage to the highly salient regions than multiplication of the two maps.

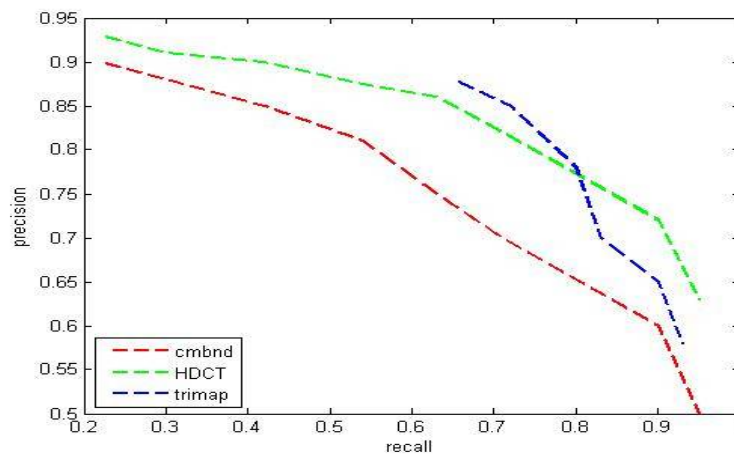


Fig.2 comparison of precision recall curve of each step on MSRA dataset

IV. BENCH MARK DATA SETS

1) **MSRA-B Dataset:** The MSRA-B salient object dataset contains many images with the pixel-wise ground truth used by the authors provided by Jiang et al. . This dataset mostly contains comparatively salient objects in which the colors are definitely different from the background, and therefore, it is considered a less challenging dataset for salient object. For the original input image from Fig.3 we can observe color transform image, final segmented tri-map and also we get final extracted salient map for MSRA-B Dataset.

MSRA Dataset Result

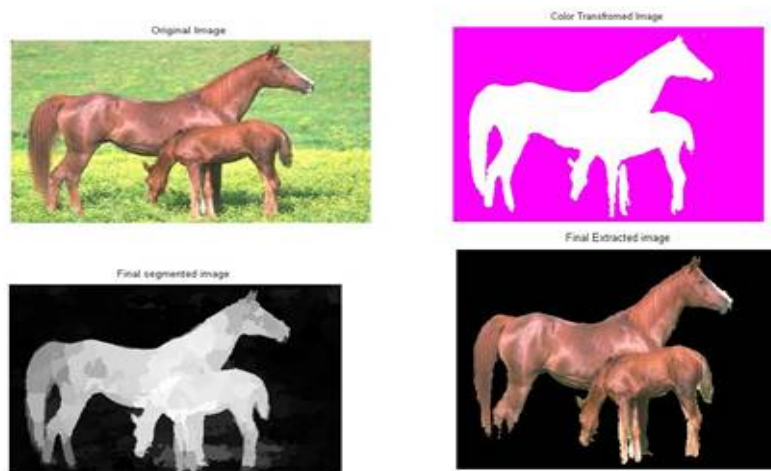


Fig. 3 MSRA dataset result

International Journal of Innovative Research in Computer and Communication Engineering

(An ISO 3297: 2007 Certified Organization)

Website: www.ijircce.com

Vol. 5, Issue 7, July 2017

2)ECSSD Dataset: The ECSSD dataset contains many images that include multiple salient objects[3] with structurally complex backgrounds that make the detection task much more challenging, such as a green apple on a tree or a yellow butterfly on yellow flowers. In addition, many images contain a single salient object with multiple colors, making it harder to detect the salient object entirely. . For the original input image from Fig. 4 we can observe color transform image, final segmented tri-map and also we get final extracted salient map for ECSSD Dataset.

ECSSD Dataset Result



Fig. 4 ECSSD Dataset Result

3)PASCAL-S Dataset: The PASCAL-S dataset contains many images with multiple objects in a single image with pixel-wise ground-truth annotations. This dataset [3]provides both fixations and salient object annotations. However, this dataset is challenging as it contains many test images with very large or very small salient objects that are relatively difficult to detect entirely. . For the original input image from Fig. 5 we can observe color transform image, final segmented tri-map and also we get final extracted salient map for PASCAL Dataset.

PASCAL dataset Result

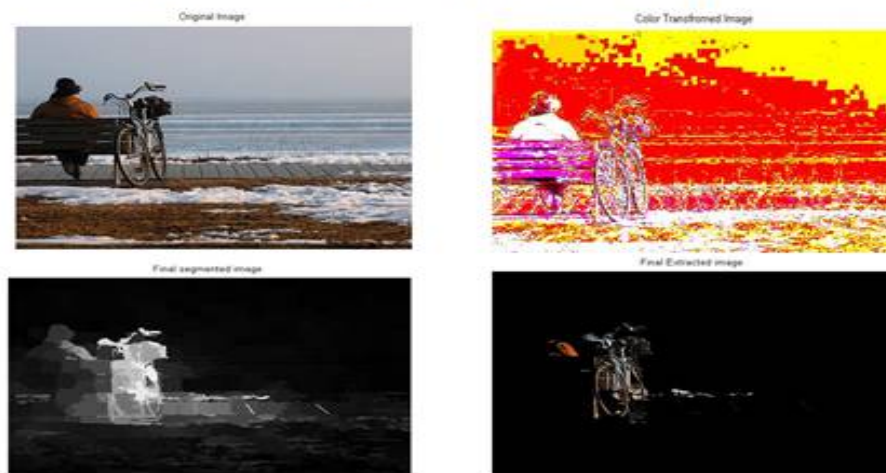


Fig.5 PASCAL-S Dataset Result

International Journal of Innovative Research in Computer and Communication Engineering

(An ISO 3297: 2007 Certified Organization)

Website: www.ijircce.com

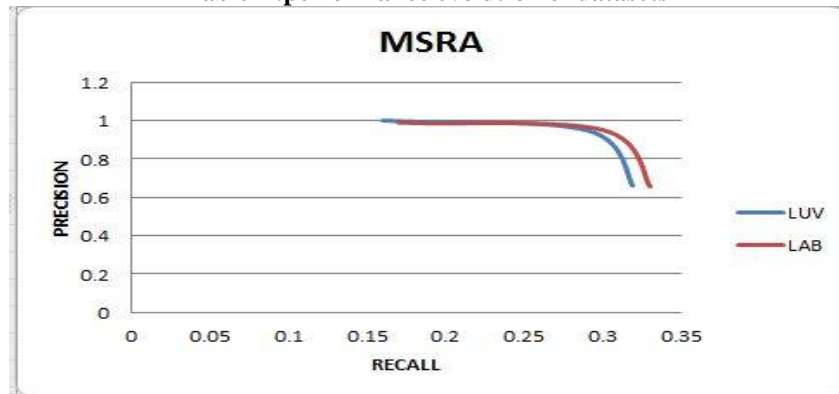
Vol. 5, Issue 7, July 2017

V. PERFORMANCE EVALUATION

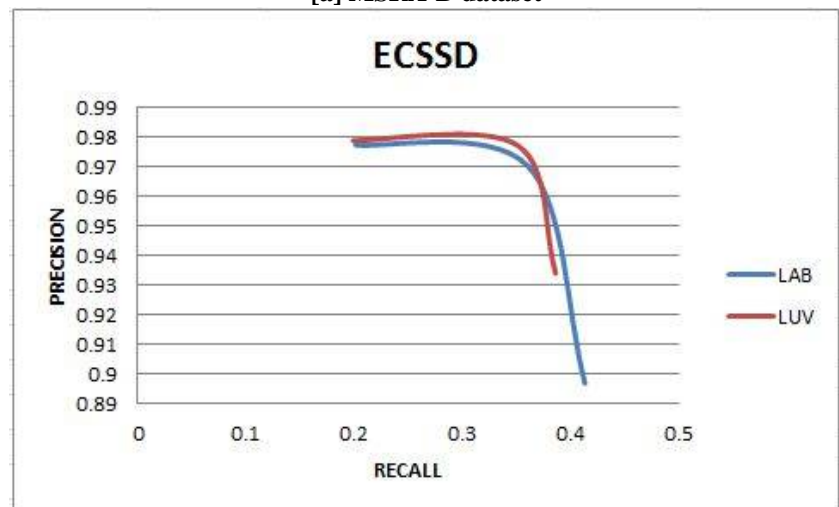
To evaluate the effectiveness of our saliency estimation, from Fig. 6 we compared the precision-recall curve with lab and luv color space on three representative benchmark datasets with the precision-recall values obtained from the performance evolution of datasets Table.1. Therefore from that we observe luv color space is more efficient compared to lab color space. Where precision also called positive predictive value. Recall also known as sensitivity.

DATA SET	PRECISION		RECALL	
	LAB	LUV	LAB	LUV
MSRA	0.9899	0.9999	0.3305	0.3290
ECSSD	0.8967	0.9338	0.4135	0.3863
PASCAL	0.9858	0.9970	0.0467	0.0495

Table 1 .performance evolution of datasets



[a] MSRA-B dataset



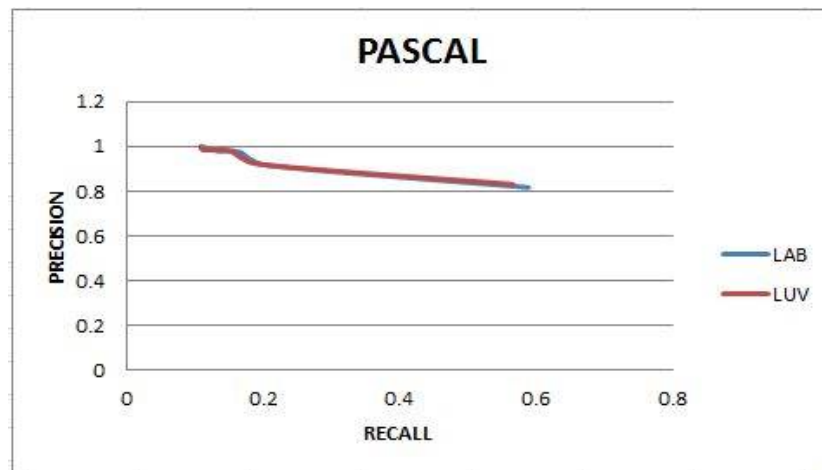
[b] ECSSD dataset

International Journal of Innovative Research in Computer and Communication Engineering

(An ISO 3297: 2007 Certified Organization)

Website: www.ijircce.com

Vol. 5, Issue 7, July 2017



[c] PASCAL dataset

Fig. 6 Comparison of the precision-recall curve with lab and luv color space on three representative benchmark datasets: [a]. MSRA-B dataset, [b]. ECSSD dataset, and [c]. PASCAL-S dataset.

VI. CONCLUSION

We have presented a novel salient region detection method that estimates the foreground regions from a trimap using two different methods: global saliency estimation via LUV Color space and local saliency estimation via regression. The trimap-based robust estimation overcomes the limitations of inaccurate initial saliency classification. Here we compared the performance evolution of MSRA, ECSSD, PASCAL datasets using Lab and Luv color space. As a result, our method luv achieves good performance and is computationally efficient in comparison to the lab method. Which is the best performing method for salient region detection of an image with better Precision-recall values. Therefore we extended the features for the initial trimap by using luv color space.

REFERENCES

- [1]. R. Achanta, A. Shaji, K. Smith, A. Lucchi, P. Fua, and S. Süsstrunk, "SLIC superpixels compared to state-of-the-art superpixel methods," *IEEE Trans. Pattern Anal. Mach. Intell.*, vol. 34, no. 11, pp. 2274–2282, Nov. 2012.
- [2]. J. Kim, D. Han, Y.-W. Tai, and J. Kim, "Salient region detection via high-dimensional color transform," in *Proc. IEEE Conf. Comput. Vis. Pattern Recognit. (CVPR)*, Jun. 2014, pp. 883–890.
- [3]. A. Borji, M.-M. Cheng, H. Jiang, and J. Li. (2014). "Salient object detection: A survey." [Online]. Available: <http://arxiv.org/abs/1411.5878>
- [4]. A. Borji, M.-M. Cheng, H. Jiang, and J. Li. (2015). "Salient object detection: A benchmark." [Online]. Available: <http://arxiv.org/abs/1501.02741>
- [4]. H. Andrews and C. Patterson, "Singular value decompositions and digital image processing," *IEEE Trans. Acoust., Speech, Signal Process.*, vol. 24, no. 1, pp. 26–53, Feb. 1976.
- [5]. M.-M. Cheng, G.-X. Zhang, N. J. Mitra, X. Huang, and S.-M. Hu, "Global contrast based salient region detection," in *Proc. IEEE Conf. Comput. Vis. Pattern Recognit. (CVPR)*, Jun. 2011, pp. 409–416.
- [6]. P. K. Kaiser and R. M. Boynton, *Human Color Vision*, 2nd ed. Washington, DC, USA: OSA, 1996.
- [7]. A. Borji, D. N. Sihite, and L. Itti, "Salient object detection: A benchmark," in *Proc. IEEE Eur. Conf. Comput. Vis. (ECCV)*, Oct. 2012, pp. 414–429.
- [8]. D. A. Klein and S. Frntrop, "Center-surround divergence of feature statistics for salient object detection," in *Proc. IEEE Int. Conf. Comput. Vis. (ICCV)*, Nov. 2011, pp. 2214–2219.
- [9]. A. Borji and L. Itti, "Exploiting local and global patch rarities for saliency detection," in *Proc. IEEE Conf. Comput. Vis. Pattern Recognit. (CVPR)*, Jun. 2012, pp. 478–485.
- [10] N. Otsu, "A threshold selection method from gray-level histograms," *IEEE Trans. Syst., Man, Cybern.*, vol. 9, no. 1, pp. 62–66, Jan. 1979.